J Nanopart Res (2018) 20: 58
https://doi.org/10.1007/s11051-018-4164-z

RESEARCH PAPER

Charge-doping and chemical composition-driven magnetocrystalline anisotropy in CoPt core-shell alloy clusters

P. Ruiz-Díaz · M. Muñoz-Navia · J. Dorantes-Dávila

Received: 6 November 2017 / Accepted: 13 February 2018 / Published online: 28 February 2018

Abstract Charge-doping together with 3*d*-4*d* alloying emerges as promising mechanisms for tailoring the magnetic properties of low-dimensional systems. Here, throughout ab initio calculations, we present a systematic overview regarding the impact of both electron(hole) charge-doping and chemical composition on the magnetocrystalline anisotropy (MA) of CoPt core-shell alloy clusters. By taking medium-sized Co_nPt_m ($N = n + m = 85$) octahedral-like alloy nanoparticles for some illustrative core-sizes as examples, we found enhanced MA energies and large induced spin(orbital) moments in Pt-rich clusters. Moreover, depending on the Pt-core-size, both in-plane and off-plane directions of magnetization are observed. In general, the MA of these binary compounds further stabilizes upon charge-doping. In addition, in the clusters with small MA, the doping promotes magnetization switching. Insights into the microscopical origins of the MA behavior are associated to changes in the electronic structure of the clusters.

P. Ruiz-Díaz (✉) · J. Dorantes-Dávila
Instituto de Física, Universidad Autónoma de San Luis Potosí, 78000 San Luis Potosí, México
e-mail: prudi@ifisica.uaslp.mx

M. Muñoz-Navia
CONACyT-Instituto de Física, Universidad Autónoma de San Luis Potosí, 78000 San Luis Potosí, México

Keywords Charge-doping · CoPt core-shell alloy clusters · Ab initio calculations · Magnetic anisotropy · Binary nanoalloys · Modeling and simulation

Introduction

The magnetic properties exhibited in nanostructures made of just a few atoms are usually very different in comparison with the ones observed in bulk, surfaces, or thin-films (Bergman et al. 2016; Pianet et al. 2016; Cui et al. 2016; Singha et al. 2016; Li et al. 2016; Donati et al. 2016; Loth et al. 2012). In general, they are difficult to predict because they depend on countless number of factors such as chemical composition (Díaz-Sánchez et al. 2013), shape, size (Gruner et al. 2008), symmetry, magnetic ordering (Ruiz-Díaz et al. 2015), and interactions with its surroundings (Serrate et al. 2016), to name just a few. Nevertheless, there is currently a large number of cutting-edge experimental techniques which allow to characterize, manipulate, and fabricate magnetic nanostructures atom by atom from bottom-up approaches (Meier et al. 2008; Rau et al. 2014; Donati et al. 2014; Khajetoorians et al. 2012). From a fundamental perspective, the manipulation and control of these nanostructured materials allow us to study the underlying interactions that govern the magnetic phenomena at the atomic scale which are the essential ingredients to form the basis

in the designing and developing of novel storage technologies with specific functionalities (Jungwirth et al. 2016; Loth et al. 2012; Khajetoorians et al. 2011).

In particular, transition-metal(TM)-based nanoparticles have been spotlighted due to a variety of technological applications(Sun et al. 2000; Yin et al. 2007; Sahoo et al. 2010). For instance, large magnetic anisotropy energies (MAEs) in small aggregates are often reported and it is of paramount importance bearing in mind that the MAE defines a preferential direction of magnetization and stabilizes such direction against temperature and external fields. The 3*d*-5*d* alloying is one of most widely used techniques for tuning the magnetic properties of small nanoparticles. It combines the large and stable magnetic moments of the strongly ferromagnetic 3*d* elements (e.g., Fe, Co, or Ni) with highly polarizable 5*d* elements such as Pt or Ir which often yields in a remarkable enhancement of the MAE in comparison with single-element compounds. For instance, combined theoretical and experimental works on relatively large-sized 3*d*-5*d*(4*d*) alloy core-shell clusters $\sim$ 43–500 atoms in CoRh (Muñoz-Navia et al. 2009; Muñoz-Navia et al. 2009; Díaz-Sánchez et al. 2013) and FePt, CoPt nanoparticles $\sim$ 13–920 atoms (Gruner et al. 2008; Gruner 2010) respectively have been highlighted the strong dependence of the magnetic properties on the chemical composition and cluster-shape. Altogether, enhanced anisotropies along with large orbital moments are remarked upon alloying for these binary compounds. Bimetallic compounds are also of great interest due to their lattice mismatch; strain-induced effects in core-shell nanoparticles have been reported which may play an important role into their local properties (Panizon and Ferrando 2016). For instance, core-shell morphologies have been produced experimentally to exploit the lattice strain to tune their chemical properties as in the case of PtCu-Pt nanoparticles (Strasser and Koh 2010).

In addition to varying the chemical composition to tune the electronic environment of the nanoalloys, there are alternative mechanisms which also allow to alter their electronic and magnetic properties. It is among the most popular approaches one can mention for instance the electric and magnetic field-assisted methods (Dasa et al. 2013, 2012; Hsu et al. 2017), being the former one of particular interest due to its local nature. However, this may involve the usage of external sources to generate such fields which is a clear disadvantage. Interestingly, a thoroughly used method in electrochemistry (Gleiter et al. 2001; Schnur and Groß 2011) but little exploited in the context of low-dimensional systems to tailor the local electronic properties is through the change in the carrier density or charge-doping. Recently, electron-doping has been proposed as a promising route to alter the magnetic properties of nanostructured materials in a controlled fashion. For instance, it has been shown that in ultra-thin multilayered systems (Ruiz-Díaz et al. 2013; Ruiz-Díaz and Stepanyuk 2014), the anisotropy is deeply modified upon electron(hole)-doping and triggers magnetization switching.

The objective of this work is to perform a *first-principles* calculations to investigate the impact of both chemical composition and charge-doping on the magnetic properties of TM binary nanoparticles taking CoPt core-shell alloys as prototypical examples. Notice that more complex configurations such as intermixing structures are also possible (Panizon and Ferrando 2016). Yet, our optimization procedure (initial core-shell like structures with no lattice mismatch only allows us to explore local minima, i.e., we exclude the possibility of taking into account other low-symmetry structures (Rossi et al. 2008; Barcaro et al. 2010). However, the validity and main conclusions regarding the influence of both chemical composition and charge doping on the magnetic properties of binary clusters will remain. Indeed, we demonstrate that the appropriate combination of 3*d* and 5*d* elements allows us to merge large moments with large MAEs. Moreover, charge-doping further stabilizes the MAE and boosts magnetization switching processes. The remainder of the paper is organized as follows: First, we highlight the main aspects regarding the theory and computations details used in the presented calculations. Later, we discuss the charge-doping effects and the impact of composition on the magnetic properties of CoPt core-shell alloys and correlate the MAE behavior with changes in the electronic structure of the clusters due to an enhancement of the spin-orbit interactions upon increasing the Pt-core-size. Finally, some general conclusions are outlined.

Computational details

The ground-state magnetic properties of the Co_nPt_m core-shell alloy clusters are obtained in the framework

of Hohenberg-Kohn-Sham's density functional theory (DFT) (Hohenberg and Kohn 1964; Kohn and Sham 1965) as implemented in the *Vienna Ab initio Simulation Package* (VASP) (Kresse and Furthmüller 1996; Kresse and Hafner 1993). The spin-polarized Kohn-Sham (KS) equations (Kohn and Sham 1965) are solved in an augmented plane-wave basis set by using the projector augmented wave (PAW) method (Blöchl 1994; Kresse and Joubert 1999) within the supercell approach. For $3d$–$5d$ TM binary alloys, the electronic and magnetic properties are accurately described by considering the $5d$, $5s$ and $3d$, $4s$, and $4p$ electrons as valence states respectively (Blöchl 1994; Kresse and Joubert 1999). The exchange and correlation effects are treated in the generalized-gradient (GGA) (Parr and Yang 1989; Dreizler and Gross 1990) level by means of the Perdew-Wang exchange-correlation functional (PW91) (Perdew 1991). The clusters are placed inside of a simple cubic supercell whose dimensions are such that the interactions between neighboring images are negligible. In practice, this criterion is fulfilled when the images are separated from each other by at least 12 Å. The KS wave functions in the interstitial region are expanded in a plane wave basis set with a kinetic energy cutoff of 350 eV. Larger supercell sizes and higher cutoff energies were also tested yielding variations in the total energy less than 1 meV/per atom. Thus, the set of values chosen for supercell size and energy cutoff in the present work represent a good compromise between computational effort and accuracy. A modest Gaussian smearing (Mermin 1965) of the KS levels of 0.01 eV is introduced in order to improve the convergence and numerical stability. The energy calculations are carried out by considering only the Γ-point in reciprocal space given that we are dealing with free-standing isolated clusters.

Structural optimization of Co_nPt_m nanoparticles

The geometry optimization of the different Co_nPt_m alloy clusters is performed by using the conjugate-gradient method until the forces on each atom are less than 5 meV/Å. The magnetic properties of the clusters are strongly dependent on the geometrical and chemical environment. Atomistic and DFT studies have predicted that in the case of core-shell nanoalloys, the lattice mismatch between elements induces a stress in the surface of the binary nanoparticles which leads in a reconstruction of the surface (Panizon and Ferrando 2016). In the case of CoPt nanoalloys, the lattice mismatch is meaningful. Typically, the nearest neighbour (NN) distance of pure-Co nanoparticles is around $d_{NN} \approx 2.3$–2.5 Å while $d_{NN} \approx 2.6$–2.8 Å for Pt-pure clusters. Thus, a careful global optimization is necessary to determine the true ground-state structure. In our study, the strain-induced effect in the restructuring of the surface is clearly observed in the case of the $Pt_{19}Co_{66}$ structure (a Pt-core surrounded by a single Co-atomic layer shell in which one observes a complex structural distortion not only in the surface but in the atoms of the inner shell as well). The atoms located in the vertices of the quadrangular face (xy-plane) are compressed regarding the ones located in the vertices of the z-axis, generating an egg-like structure. The other considered CoPt morphologies (intermixed structures) also undergo non-trivial distortions. It is worthy to point out that such geometrical reconstruction breaks the overall symmetry of the structure suppressing the usual high-symmetry axes found in the conventional systems (e.g., cubic, hexagonal symmetry).

Since the magnetic degrees of freedom rise (existence of multiple magnetic configurations) when the number of atoms in the cluster increases, we consider a wide-range of possible collinear solutions as starting magnetic configurations having different spin arrangements for the cluster geometry optimizations. A structural optimization alongside with a systematic search of collinear magnetic solutions following a fixed-spin-moment procedure is performed by varying the total spin moment S_z of the cluster around some reasonable values $N < S_z < 3N$. Moreover, small random variations of the atomic positions and local moment orientations are introduced (non-collinear textures), which allows to test the stability of collinear solutions. The collinear spin-magnetic-moment configurations turned out to be the ground-state textures in all cases upon geometry and energy optimization.

Charge-doping and magnetocrystalline anisotropy

Once the ground-state structures of the Co_nPt_m nanoparticles are obtained, we introduce a uniform charged-background inside of the supercell in order to simulate the charge-doping effect on the clusters (Ruiz-Díaz and Stepanyuk 2014). In practice, this can be achieved by varying the total number of valence

electrons of the Co_nPt_m nanoparticles. Typically, by adding(removing) one electron in the supercell with respect to the non-charged cluster (reference system) is enough for simulating a reasonable electron(hole)-doping. Clearly, the excess of charge(holes) causes the neutrality condition in the supercell to be broken. Thus, the excess of charge needs to be compensated by a constant background jellium to fulfill this constraint, otherwise the Coulomb energy would diverge (Gerstmann et al. 2003). This approach has been successfully applied in our previous works for ultra-thin multi-layered systems (Ruiz-Díaz et al. 2013; Ruiz-Díaz and Stepanyuk 2014). The magnetocrystalline anisotropy energy is a very sensitive quantity which requires to be treated with extreme care since for free-standing isolated clusters is usually of the order of just a few meV's. In a second step, relativistic calculations taking into account the *spin-orbit* interaction are carried out with a much tight criterion in the electronic energy($\Delta E = 10^{-7}$ eV between two successive electronic steps). Such a strict criterion is crucial for calculating reliable MAEs. We rely on the magnetic force theorem (Bruno 1989) for determining the MAE of the clusters. Self-consistent calculations were also performed finding in both cases the same trends in the MAE behavior however. One should mention that the spin and orbital moments remain collinear between each other in both approaches (non-self and fully self-consistent relativistic calculations). We therefore focus our discussion mainly in the results obtained with the former approach.

Results and discussion

Non-charged CoPt clusters

We take as prototypical examples medium-sized CoPt octahedral-like core-shell alloy clusters having $N = n + m = 85$ atoms and different core sizes, $\eta_c = N_c/N = 0.23$, 0.5, 0.72 and 1.0 where N_c is the number of atoms in the core. The considered CoPt core-shell structures are sketched in Fig. 1. We begin our study by analyzing the role of the structural relaxations in the nanoparticles. In general, upon geometry optimization, the Co_nPt_m alloys try to preserve their initial symmetry (octahedral symmetry) but noticeable distortions near the apexes are observed, specially in the case of $Pt_{19}Co_{66}$ when an egg-like structure

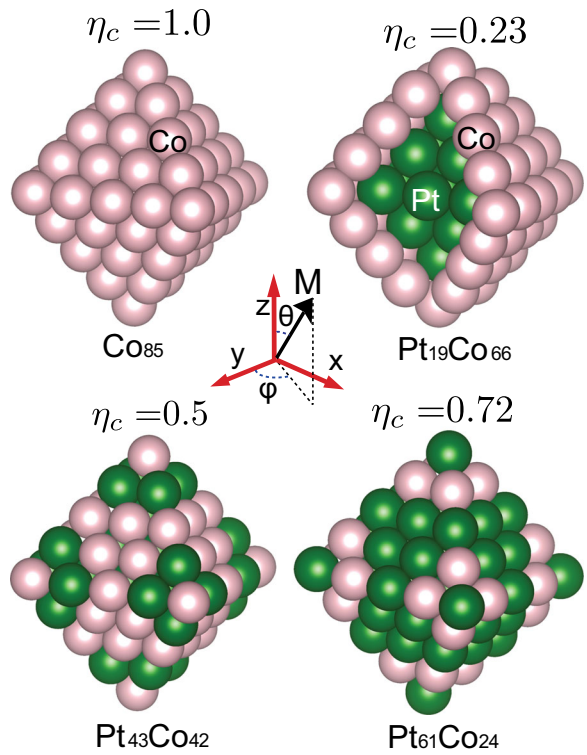

Fig. 1 (Color online) Illustration of the relaxed Co_nPt_m octahedral-like core-shell alloy clusters having $N = n + m = 85$ atoms and different relative core sizes $\eta_c = N_c/N$, where N_c is the number of atoms in the core. Light (pink) balls represent the Co atoms while dark (green) balls represent the Pt atoms

is formed. Only for the case of the pure Co-cluster (Co_{85}), shorter inter-atomic distances are found in comparison to the nearest-neighbors distance in bulk [$d = (2.35–2.44)$Å; $d^{Co}_{bulk} = 2.49$Å]. For the CoPt alloys, the displayed inter-atomic distances are in the range of bulk distances $d = (2.37\text{-}2.92)$Å for $Pt_{19}Co_{66}$, $d = (2.43\text{-}2.84)$Å for $Pt_{43}Co_{42}$, and $d = (2.49–2.77)$Å for $Pt_{61}Co_{24}$ respectively. In order to get insights regarding the stability of the selected CoPt morphologies, we calculate the binding energy per atom (E_{bin}) in the canonical way: $E_{bin} = 1/N \times (E_{tot} - nE_{Co} - mE_{Pt})$ where $N = 85$, E_{tot} is the total energy of the cluster Co_nPt_m and $E_{Co}(E_{Pt})$ is the energy of an single Co and Pt-atom respectively. We found $E_{bin}(Co_{85}) = -4.48$ eV, $E_{bin}(Pt_{19}Co_{66}) = -4.4$ eV, $E_{bin}(Pt_{43}Co_{42}) = -4.6$ eV, $E_{bin}(Pt_{61}Co_{24}) = -4.71$ eV. From such results, one concludes that the inter-mixed structures are lower in energy than that of the core-shell morphology. Even the pure Co-cluster (Co_{85}) turned to be more stable than $Pt_{19}Co_{66}$. These

results are in agreement with previous calculations using Monte Carlo and DFT methods for global optimization of structures in CoPt nanostructures which predict that the the intermixing is prefered for this kind of nanoalloys (Rossi et al. 2008; Barcaro et al. 2010).

Now that different Pt-Co intermixing substitutions are considered, the magnetic behavior is expected to be highly composition-dependent to the chemical order. In particular, we focus in striving to correlate the magnetocrystalline anisotropy with the chemical composition of the nanoparticle. Due to the symmetry of the selected clusters, the energy is calculated along the three highest symmetry magnetization directions (see Fig. 1), namely $\delta = x, z$ and $xy := \{\phi = \pi/4, \theta = \pi/2\}$ for each considered core size, η_c. As briefly discussed before, due to the lattice mismatch between Co and Pt, the structural distortions are considerable, breaking in this way the symmetry of the system. Therefore, the z and xy magnetization directions are non-equivalent otherwise this should be the case (i.e., perfect octahedral cluster). From these calculations, two magnetic anisotropy energies are obtained. An in-plane anisotropy which is the difference in energy between the xy and x directions, $\Delta E_{in} = E_{xy} - E_x$ and an out-of-plane anisotropy defined by difference in energy between the z and x directions, $\Delta E_{out} = E_z - E_x$ respectively. Owing to the symmetry of the considered clusters, we found that the out-of-plane MAEs are in general larger than the in-plane MAEs. For sake of sampling further the MAE behavior, an additional direction of magnetization was chosen. We take the $xz := \{\phi = 0, \theta = \pi/4\}$ direction, finding a considerable monotonous increasing of the MAE upon Pt-to-Co substitution. Defining now ΔE as $E_z - E_{xz}$, we obtain $\Delta E = 0.41, -91.23, -205.47$, and -332.6 meV for Co_{85}, $Pt_{19}Co_{66}$, $Pt_{43}Co_{42}$, and $Pt_{61}Co_{24}$ respectively. In order to get insights regarding the influence of the structural distortions on the MAE, we calculate as an example ΔE_{out} for the non-distorted $Pt_{19}Co_{66}$ morphology assuming $d = 2.68$ Å between all the atoms. In this case, ΔE_{out} is -9.2 meV which is relative larger than that of the MAE of the optimized cluster (≈ 6 meV). In general, enhanced MAEs are observed in the non-distorted structures exhibiting that relaxations tend to reduce the MAE value.

We have obtained the energy along three different axes of quantization, the directions along the corner, center of edge and center of facet of the clusters; however, in order to determine the *true* hard axis or global minimum, one needs to calculate the energy in all the magnetization axes, namely $E(\phi, \theta)$ which is beyond the scope of the present study. We mainly focus on the trends of the MAE as a function of the chemical composition and charge doping.

Moreover, the effect of the $3d$-$5d$ alloying on the MAE is exhibited since enhanced MAEs are obtained as the Pt-core-size increases (Pt-to-Co substitution.) We observe that among the considered Co_nPt_m core-shell clusters, the pure Co-cluster(Co_{85}) has a negligible (almost zero) MAE due to its small *spin-orbit* constant. In contrast, a non-trivial dependence of the MAE as a function of the Pt-concentration is observed. We found that the largest Pt-core-size cluster, $\eta_c = 0.72$ ($Pt_{61}Co_{24}$), possesses a remarkable large off-plan e MAE of $\Delta E_{out} = -22.9$ meV. In the xy-plane, the easy-axis of magnetization is along the $\delta = xy$ direction ($\Delta E_{in} = -23.6$ meV). In addition, depending on the Pt-core-size, both in-plane(off-plane) directions of magnetization are identified as it can be seen in Fig. 2.

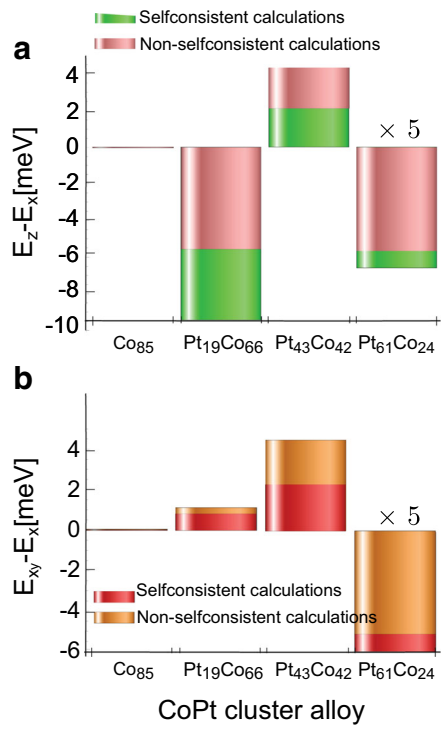

Fig. 2 (Color online) Calculated self-consistent (SC) and non-self-consistent (NSC) magnetocrystalline anisotropy energy of Co_nPt_m core-shell clusters having $N = n + m = 85$ atoms and different core sizes η_c. **a** Out-of plane anisotropy $\Delta E = E_z - E_x$. **b** In-plane anisotropy $\Delta E = E_{xy} - E_x$. The units are given in meV.

Therefore, the strong chemical composition dependence on the magnetization direction is evidenced. The results show that this non-trivial MAE behavior renders impossible to a priori infer a clear trend of the MAE based only on the chemical composition of the cluster. This intricate behavior arises from the interplay of the local environment dependence and the corresponding enhancement of spin-orbit interactions.

We would like to comment in brief on the reliability of the approach used in calculating the MAEs. In general, the magnetic properties, in particular the MAE, are very sensitive to countless factors and certainly different levels of accuracy might yield to varied values. In order to quantify to some extend the robustness of the approach embraced in the present work, we compare both self-consistent and non-self consistent (magnetic force theorem) calculations for the non-charged clusters. We find that the general trends in the MAE behavior are preserved in *all* the considered cases (see Fig. 2). Thus, the magnetic properties of the charged CoPt clusters are discussed using the magnetic force theorem since we expect that the conclusions should remain the same.

In Table 1, the average magnetic spin and orbital moments as well as the corresponding local Co(Pt) moments for the different Co_nPt_m core-shell alloy clusters are presented. In the pure Co-cluster (Co_{85}), the average magnetic moment is modestly larger ($\bar{\mu} = 1.78\ \mu_B$) than that in the bulk. On the other hand, although the average spin moment, $\bar{\mu}$, of the cluster decreases as a whole when increasing the Pt-core-size from $\eta_c = 0.23$ to 0.72, thanks to the increase of the contact with the Pt-atoms, the local spin moment of the Co atoms increases from 1.78 to 2.06 μ_B. Consequently, owing to an enhancement in the hybridization of the Pt atoms, the induced spin moment slightly increases from 0.36 to 0.48 μ_B. The orbital moments in the Co atoms are practically negligible regardless of the concentration of Pt in the cluster. Contrary, it is observed a dependence on the chemical composition of the nanoparticles in the orbital moments of the Pt atoms with small variations ranging from 0.01–0.2 μ_B.

Charged CoPt clusters

The MAE in the CoPt alloys can be further altered by electron(hole)-doping. The excess(lack) of charge modifies the intra-atomic Coulomb repulsion that yields in a electronic redistribution affecting the MAE value. In between, such redistribution might also cause structural deformations in the nanoparticles. We found that in general such distortions are negligible for the considered electron(hole)-doping strength [1 electron(hole) per unit-cell]. Variations less than 2% in the interatomic distance with respect to the non-charge systems are observed. As in the case of the non-charged alloy nanoparticles, we calculate the energy of the clusters along the three highest symmetry axes as a function of the electron(hole)-doping strength. We start by discussing the results for the in-plane MAE ($\Delta E_{in} = E_{xy}$-E_x) which are summarized in Fig. 3. Enhanced MAEs upon charge-doping are obtained in all the cases along with a non-monotonous MAE behavior as a function of function of the electron(hole)-doping strength. Interestingly, in

Table 1 Average spin(orbital) magnetic moments in core-shell Co_nPt_m clusters having N= $n + m = 85$ atoms

	$\bar{\mu}$	$\bar{\mu}_{Pt}^{WS}$	$\bar{\mu}_{Co}^{WS}$	$\bar{\mu}_L^z$	$\bar{\mu}_L^x$	$\bar{\mu}_L^{xy}$	$\bar{\mu}_L^{Pt}$	$\bar{\mu}_L^{Co}$
Co_{85}	1.78		1.78	[0.12]	0.096	0.096		0.12
$Co_{66}Pt_{19}$	1.54	0.36	1.86	[0.092]	0.09	0.087	0.05	0.095
$Co_{42}Pt_{43}$	1.18	0.39	2.0	0.097	[0.1]	0.097	0.132	0.17
$Co_{24}Pt_{61}$	0.82	0.48	2.06	[0.06]	0.068	0.064	0.2	0.01
Co_{fcc}	1.65							
Pt_{fcc}	0.0							

Results are given for the average spin moment per atom within the Wigner-Seitz (WS) spheres $\bar{\mu}^{WS} = \sum_{i=1}^{N} \mu_i/N$ (column 2), the average Pt magnetic moment $\bar{\mu}_{Pt}^{WS} = \sum_{i=1}^{m} \mu_i^{Pt}/m$ (column 3), and the average Co magnetic moment $\bar{\mu}_{Co}^{WS} = \sum_{i=1}^{n} \mu_i^{Co}/n$ (column 4). Columns 5, 6, and 7 refer to the average orbital moment per atom ($\bar{\mu}_L^{\delta} = \sum_{i=1}^{N} \mu_L^{\delta}(i)/N$) in $\delta = z, x, xy$ directions respectively. Columns 8 and 9 stand for the Pt[Co] orbital moment in easy-axis of magnetization (the easy-axis direction is marked in brackets), $\bar{\mu}_L^{Pt} = \sum_{i=1}^{m} \mu_L(Pt)_i/m$[$\bar{\mu}_L^{Co} = \sum_{i=1}^{n} \mu_L(Co)_i/n$]. The orbital magnetization directions $\delta = \{z, x, xy\}$ are chosen following the high-symmetry axes of the CoPt-clusters according to Fig. 1. For sake of reference, the corresponding bulk values are also shown

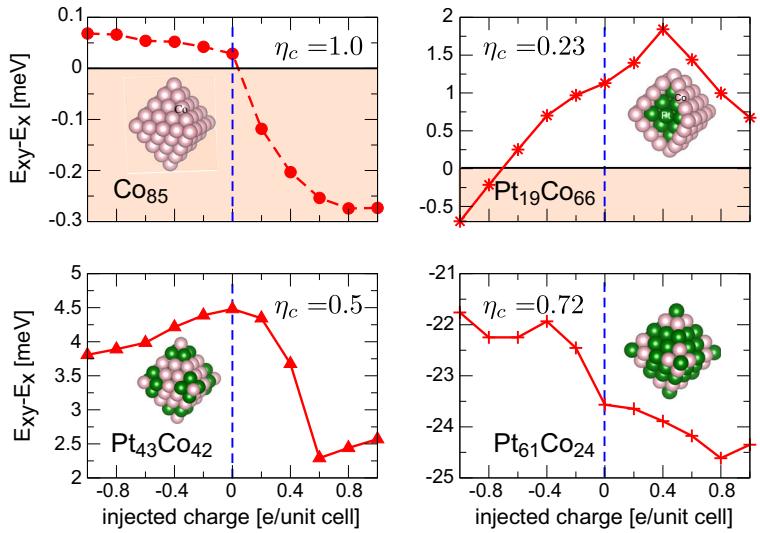

Fig. 3 (Color online) In-plane magnetocrystalline anisotropy $\Delta E = E_{xy} - E_x$, as a function of the electron(hole) charge-doping of the considered Co_nPt_m core-shell clusters having $N = n + m = 85$ atoms and different core sizes η_c. The charge-doping scale (in units of e/unit cell) is referred to the neutral system. Positive (negative) values stand for an excess(lack) of valence electrons in the alloy cluster

the Co-rich nanoparticles regime (Co_{85} and $Pt_{19}Co_{66}$) magnetization switching is reveal (Fig. 3a–b). This is due to the relative small displayed in MAEs ($\sim$ 0.1-1.5 meV) and under this scenario, the doping plays a key role over the competing weak magnetic interactions driven by the spin-orbit coupling. When increasing the Pt-concentration in the clusters, larger in MAEs are obtained ($\sim$2.5$-$24 meV for $\eta_c = 0.5, 0.72$) (Fig. 3c–d) and the magnetization switching mechanism is suppressed. Comparing our results, we can conclude that Co-to-Pt substitution promotes further stabilization mediated by the spin-orbit interactions.

Let us move the discussion to the results regarding the off-plane MAE in the CoPt core-shell alloys. First of all, the same qualitative tendency (similar non-monotonous dependence of the MAE as a function of the charge-doping strength) is observed in the four considered clusters; however, the obtained MAEs are larger in comparison with the in-plane MAEs previously discussed. Nonetheless, the spin-orbit constant for Co is small and the Co_{85} displays a modest in-plane MAE (neutral system); however, the changes in the MAE behavior are noticeable upon the doping. The non-charged cluster has a very small in-plane anisotropy (close to zero), so it is expected that small variations in the electronic environment will produce reversal magnetization. The easy-axis of magnetization happens to be out of plane, along the z-axis

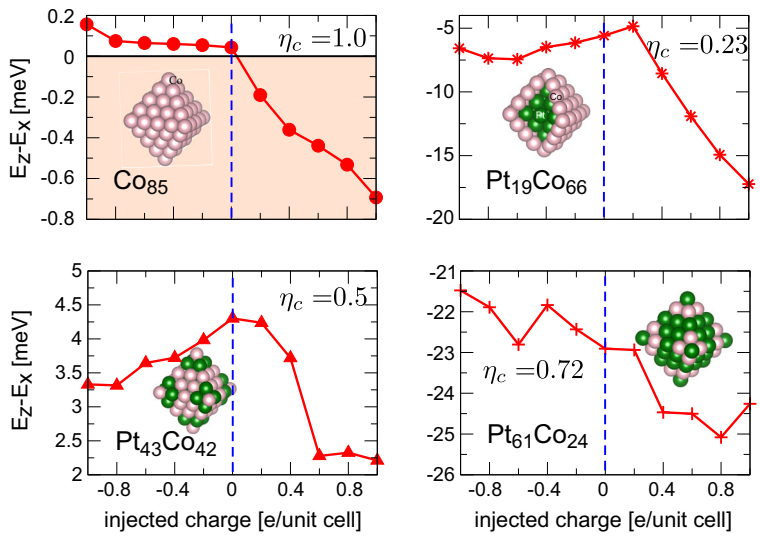

Fig. 4 (Color online) Off-plane magnetocrystalline anisotropy $\Delta E = E_z - E_x$, as a function of the electron(hole) charge-doping of the considered Co_nPt_m core-shell clusters having $N = n + m = 85$ atoms and different core sizes η_c. The charge-doping scale (in units of e/unit cell) is referred to the neutral system. Positive (negative) values stand for an excess(lack) of valence electrons in the cluster

upon charge injection and becomes more stable as the charge doping strength increases. The anisotropy further stabilizes reaching values around 0.7 meV for 1*e*/unit-cell. Contrary, it would appear that the initial weak in-plane MAE is restored and shows a linear behavior upon hole injection (see Fig. 4a). Its value is roughly constant nearly 0.1 meV with hardly appreciable variations.

A more complicated behavior is found in the CoPt core-shell alloys since there is no clear trend of a preferred direction of magnetization. Both Co-rich and Pt-rich concentrations ($\eta_c = 0.23$ and 0.73) display remarkable large off-plane MAEs exhibiting values ranging from 17 to 25 meV upon electron-doping (see Fig. 4b–d). Only in case where the ratio between the number of Co and Pt atoms is the same ($\eta_c \sim 0.5$), the nanoparticle has a relative small in-plane MAE ranging from 2.5 to 3.5 meV (see Fig. 4c). Intriguingly, for any of the studied CoPt core-shell alloys, no evidence of reversal magnetization was observed. It can be attributed to the relative large ΔE_{out} values evidencing the robustness of the magnetization direction ruled by the large spin-orbit interactions.

Given that the magnetocrystalline anisotropy mainly arises from the spin-orbit interactions, it is expected that there is a correlation between the MAE and orbital moments. Thus, as a first approach to endeavor quantifying the charge-doping effects on the MAE, we analyze the orbital moment behavior as a function of the charge-doping strength. We choose $Pt_{19}Co_{66}$ as an example since this cluster shows a non-monotonous as well as smooth MAE behavior upon doping. In Fig. 5a–b, we present the total orbital moment of the cluster alloy for the three considered directions of magnetization $\delta = x, xy$, and z respectively. It can be appreciated that the orbital moment along the z-axis remains roughly constant approximately $\mu_L^z = 7.8\ \mu_B$ for hole injection which is consistent with the observed small variations in the off-plane MAE, ($\Delta E_{out} = E_z - E_x$) around 5–7 meV. Unlike, upon charge-doping, the orbital moment rises which is reflected by a meaningful increase of the anisotropy from $\Delta E_{out} \sim 5$ to 17 meV (Fig. 4b). Similar conclusions can be deduced when comparing $\Delta E_{in} = E_{xy}$-E_x and $\mu_L^{x,xy}$. These results evidence that a change in MAE can be associated with a change in the orbital moment resembling the Bruno's relation for explaining the MAE origins (Bruno 1989). In Fig. 5c, we plot the orbital off-plane anisotropy, $\Delta\mu_L^{zx} = \mu_L^z - \mu_L^x$ as a function of the charge(hole)-doping strength. Indeed, when $\Delta\mu_L^{zx}$ raises, ΔE_{out} also increases and vice-versa.

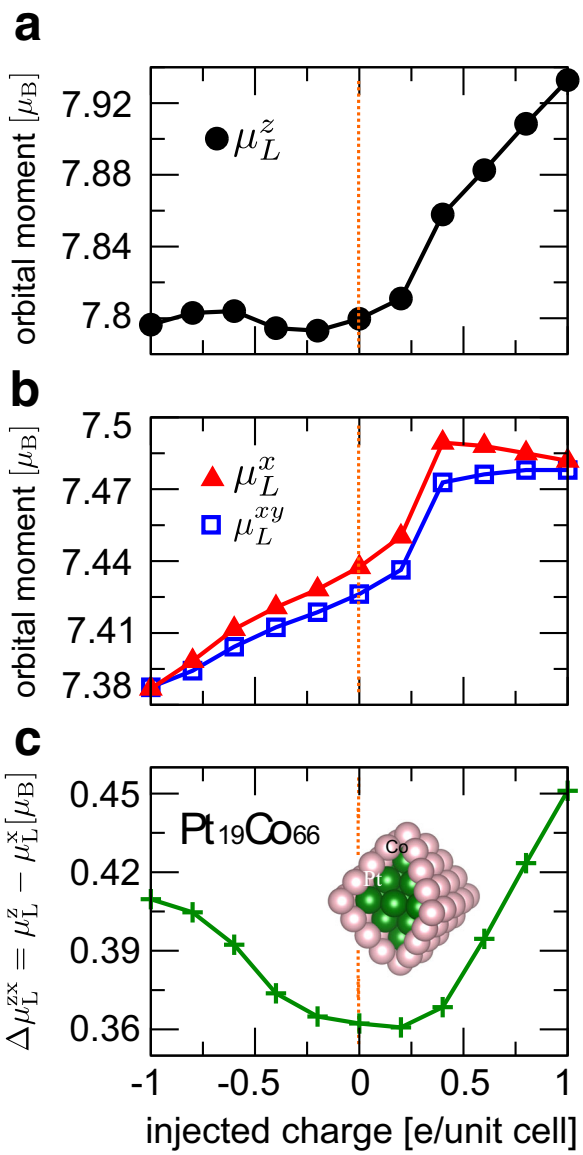

Fig. 5 (Color online) Total orbital magnetic moment $\mu_L = \sum_{i=1}^{N} \mu_i^{\delta}$, for the $Pt_{19}Co_{66}$ core-shell cluster as a function of the electron(hole) charge-doping. Positive (negative) values stand for an excess(lack) of valence electrons in the cluster. The charge-doping scale (in units of *e*/unit cell) is referred to the neutral system. **a** Total orbital magnetic moment along the z $\mu_L = \sum_{i=1}^{N} \mu_i^z$, direction according to Fig. 1. **b** Total orbital magnetic moments along $\delta = x$ and xy $\mu_L = \sum_{i=1}^{N} \mu_i^{x,xy}$, respectively. **c** Total out-of plane orbital anisotropy, $\Delta\mu_L^{zx} = \mu_L^z - \mu_L^x$. The units are given in μ_B

Table 2 Couplings between the occupied (unoccupied) states depending on the d-orbital symmetry and their contribution to the direction of magnetization

$\langle\psi_u\|\psi_o\rangle$	d_{z^2}	$d_{x^2-y^2}$
d_{xy}	~ 0	$\uparrow$
d_{xz}	$\rightarrow$	$\rightarrow$
d_{yz}	$\rightarrow$	$\rightarrow$

The vertical (horizontal) arrows referred to an off-plane(in-plane) direction of magnetization respectively. (see for instance the Supplemental Material of Ref. Ruiz-Díaz et al. (2015))

Electronic structure of the CoPt alloy clusters

A simple and fashionable way to elucidate major insights regarding the microscopy origins of the MAE behavior of the CoPt alloy clusters from a local perspective is to assess the prevailing contributions to the magnetocrystalline anisotropy driven by the coupling of the different d-orbitals with the spin-orbit angular-momentum operators. Resorting to the second-order perturbation approach (Wang et al. 1993)

$$\mathrm{MAE} = \mathrm{E_z} - \mathrm{E_x} \sim \xi^2 \sum_{o,u} \frac{|\langle\psi_u|l_z|\psi_o\rangle|^2 - |\langle\psi_u|l_x|\psi_o\rangle|^2}{\epsilon_u - \epsilon_o} \tag{1}$$

where $\{\psi_o, \psi_u\}$ refer to the unoccupied (occupied) states and $\{l_x, l_z\}$ the angular momentum operators respectively and ξ is the *spin-orbit* constant. It is straightforward to infer that the predominant contributions to the MAE arise from the states near to the Fermi level and its behavior is essentially ruled by the denominator in Eq. 1. Furthermore, since the majority d-band for the Co and Pt elements are fully occupied, the spin-flip between the up- and down-states is suppressed and the MAE behavior can be associated to the coupling between states in the minority d-band only. Depending on the symmetry of the d-orbitals, the coupling between the different occupied and unoccupied states via the spin-orbit angular-momentum operators, a particular direction of magnetization is preferred according to Table 2 (Dasa et al. 2013; Ruiz-Díaz et al. 2015). The interplay between *all* the couplings determines the easy-axis of magnetization of the cluster. In Fig. 6, the minority d-orbital-resolved density of states (DOS) for the $\mathrm{Co}_n\mathrm{Pt}_m$ core-shell alloy clusters around the Fermi level is plotted . After analyzing the spin-orbit coupling matrix elements between the different d-orbitals along with the DOS profile (DOS $\propto \langle\psi_u||\psi_o\rangle^2$), one can observed that for Co_{85}, there is a depletion of the d-orbitals near the Fermi energy (see

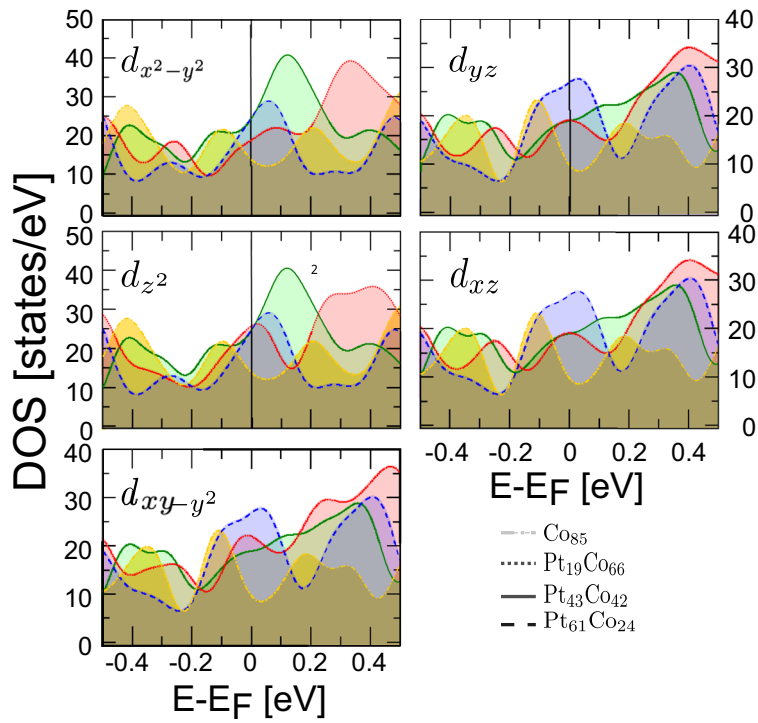

Fig. 6 (Color online) Minority d-orbital-resolved density of states(DOS) for the $\mathrm{Co}_n\mathrm{Pt}_m$ core-shell alloy clusters around the Fermi level

Fig. 6) which indicates a weak coupling between the occupied and unoccupied states yielding therefore in a negligible MAE as it was previously discussed. Contrary, the large off-plane(in-plane) MAE found for the $Pt_{61}Co_{24}$ alloy cluster($\sim$ 26 meV) can be easily understood by the substantial enhancement of the coupling mainly between the d_{xy} and $d_{x^2-y^2}$ orbitals and d_{xz} and $d_{x^2-y^2}$, which can be envisaged by the large number of of states of these orbitals around the Fermi level that favors an off-plane(in-plane) direction of magnetization respectively. The obtained intermediate MAE values ($\sim$ 2–15 meV) for the $Pt_{19}Co_{66}$ and $Pt_{43}Co_{42}$ are also reflected in the profile of the DOS for these clusters. The strength of the different off-plane(in-plane) couplings (states near the Fermi energy) are between the couplings for Co_{85} and $Pt_{61}Co_{24}$. One can see thus that the magnetocrystalline anisotropy is driven by the spin-orbit interactions and it has a profound impact in the electronic structure of the clusters which can be traced back in the density of states.

Conclusions

The magnetic properties of CoPt core-shell alloy nanoparticles have been investigated in the framework of density functional theory. Our results demonstrate that tuning the chemical composition, in particular by 3*d*-5*d* alloying and simultaneously varying their concentration has a profound impact in cluster magnetism. Remarkably, charge-doping offers an appealing route for further tailoring the magnetic properties of the cluster alloys. Our results show that this mechanism promotes further stabilization in the direction of magnetization which is appealing for instance in magnetic recording. More intriguing is that the magnetization switching processes may also be triggered. Finally, the microscopical basis of the magnetocrystalline anisotropy of the CoPt alloy clusters is associated with changes in their electronic structure and the MAE behavior can be explained qualitatively.

Acknowledgments P.R.D and M .M.N thankfully acknowledge the computer resources, technical expertise, and support provided by the Laboratorio Nacional de Supercómputo del Sureste de México (LNS). The authors also thank J. Rentería-Arriaga and J.C. Sánchez-Leaños for technical support.

Funding information J.D.D acknowledges the financial support to CONACyT trough grant 256132 and M.M.N to PROALMEX 245115.

Compliance with ethical standards

Conflict of interest The authors declare that they have no conflict of interest.

References

Barcaro G, Ferrando R, Fortunelli A, Rossi G (2010) Exotic supported copt nanostructures: from clusters to wires. J Phys Chem Lett 1(1):111–115. https://doi.org/10.1021/jz900076m

Bergman A, Hellsvik J, Bessarab PF, Delin A (2016) Spin relaxation signature of colossal magnetic anisotropy in platinum atomic chains. Sci Rep 6:36,872. https://doi.org/10.1038/srep36872

Blöchl PE (1994) Projector augmented-wave method. Phys Rev B 50:17,953–17,979. https://doi.org/10.1103/PhysRevB.50.17953

Bruno P (1989) Tight-binding approach to the orbital magnetic moment and magnetocrystalline anisotropy of transition-metal monolayers. Phys Rev B 39:865–868. https://doi.org/10.1103/PhysRevB.39.865

Cui P, Choi JH, Lan H, Cho JH, Niu Q, Yang J, Zhang Z (2016) Quantum stability and magic lengths of metal atom wires. Phys Rev B 93:224,102. https://doi.org/10.1103/PhysRevB.93.224102

Dasa TR, Ignatiev PA, Stepanyuk VS (2012) Effect of the electric field on magnetic properties of linear chains on a Pt(111) surface. Phys Rev B 85:205,447. https://doi.org/10.1103/PhysRevB.85.205447

Dasa TR, Ruiz-Díaz P, Brovko OO, Stepanyuk VS (2013) Tailoring magnetic properties of metallic thin films with quantum well states and external electric fields. Phys Rev B 88:104,409. https://doi.org/10.1103/PhysRevB.88.104409

Díaz-Sánchez LE, Dorantes-Dávila J, Pastor GM (2013) Local and chemical environment dependence of the magnetic properties of corh core-shell nanoparticles. Phys Rev B 88:134,423. https://doi.org/10.1103/PhysRevB.88.134423

Donati F, Gragnaniello L, Cavallin A, Natterer FD, Dubout Q, Pivetta M, Patthey F, Dreiser J, Piamonteze C, Rusponi S, Brune H (2014) Tailoring the magnetism of co atoms on graphene through substrate hybridization. Phys Rev Lett 113:177,201. https://doi.org/10.1103/PhysRevLett.113.177201

Donati F, Rusponi S, Stepanow S, Wäckerlin C, Singha A, Persichetti L, Baltic R, Diller K, Patthey F, Fernandes E, Dreiser J, Šljivančanin Ž, Kummer K, Nistor C, Gambardella P, Brune H (2016) Magnetic remanence in single atoms. Science 352(6283):318–321. https://doi.org/10.1126/science.aad9898

Dreizler RM, Gross EKU (1990) Density functional theory. Springer, Berlin, pp 186–187

Gerstmann U, Deák P, Rurali R, Aradi B, Frauenheim T, Overhof H (2003) Charge corrections for supercell calculations of defects in semiconductors. Phys B Condens Matter 340–342:190–194. https://doi.org/10.1016/j.physb.2003.09.111. Proceedings of the 22nd International Conference on

Defects in Semiconductors. http://www.sciencedirect.com/science/article/pii/S0921452603007592
Gleiter H, Weissmüller J, Wollersheim O, Würschum R (2001) Nanocrystalline materials: a way to solids with tunable electronic structures and properties. Acta Mater 49(4):737–745
Gruner ME (2010) Core-shell morphologies of fept and copt nanoparticles: an ab initio comparison. J Phys Conf Ser 200(7):072,039. http://stacks.iop.org/1742-6596/200/i=7/a=072039
Gruner ME, Rollmann G, Entel P, Farle M (2008) Multiply twinned morphologies of fept and copt nanoparticles. Phys Rev Lett 100:087,203
Hohenberg P, Kohn W (1964) Inhomogeneous electron gas. Phys Rev 136:B864–B871. https://doi.org/10.1103/PhysRev.136.B864
Hsu PJ, Kubetzka A, Finco A, Romming N, von Bergmann K, Wiesendanger R (2017) Electric-field-driven switching of individual magnetic skyrmions. Nat Nano 12(2):123–126. https://doi.org/10.1038/nnano.2016.234
Jungwirth T, Marti X, Wadley P, Wunderlich J (2016) Antiferromagnetic spintronics. Nat Nanotechnol 11:231–241
Khajetoorians AA, Wiebe J, Chilian B, Wiesendanger R (2011) Realizing all-spin-based logic operations atom by atom. Science 332(6033):1062–1064. https://doi.org/10.1126/science.1201725. http://www.sciencemag.org/content/332/6033/1062.abstract
Khajetoorians AA, Wiebe J, Chilian B, Lounis S, Blügel S, Wiesendanger R (2012) Atom-by-atom engineering and magnetometry of tailored nanomagnets. Nat Phys 8(6):497–503
Kohn W, Sham LJ (1965) Self-consistent equations including exchange and correlation effects. Phys Rev 140:A1133–A1138. https://doi.org/10.1103/PhysRev.140.A1133
Kresse G, Furthmüller J (1996) Efficient iterative schemes for ab initio total-energy calculations using a plane-wave basis set. Phys Rev B 54:11,169–11,186. https://doi.org/10.1103/PhysRevB.54.11169
Kresse G, Hafner J (1993) Ab initio molecular dynamics for liquid metals. Phys Rev B 47:558–561. https://doi.org/10.1103/PhysRevB.47.558
Kresse G, Joubert D (1999) From ultrasoft pseudopotentials to the projector augmented-wave method. Phys Rev B 59:1758–1775. https://doi.org/10.1103/PhysRevB.59.1758
Li J, Wang H, Hu J, Wu RQ (2016) Search for giant magnetic anisotropy in transition-metal dimers on defected hexagonal boron nitride sheet. J Chem Phys 144(20):204,704. https://doi.org/10.1063/1.4950952
Loth S, Baumann S, Lutz CP, Eigler DM, Heinrich AJ (2012) Bistability in atomic-scale antiferromagnets. Science 335(6065):196–199. https://doi.org/10.1126/science.1214131. http://science.sciencemag.org/content/335/6065/196
Meier F, Zhou L, Wiebe J, Wiesendanger R (2008) Revealing magnetic interactions from single-atom magnetization curves. Science 320(5872):82–86. https://doi.org/10.1126/science.1154415. http://www.sciencemag.org/content/320/5872/82.abstract
Mermin ND (1965) Thermal properties of the inhomogeneous electron gas. Phys Rev 137:A1441–A1443. https://doi.org/10.1103/PhysRev.137.A1441
Muñoz-Navia M, Dorantes-Dávila J, Respaud M, Pastor GM (2009) Theoretical study of the magnetic moments and anisotropy energy of corh nanoparticles. Eur Phys J D 52(1):171–174. https://doi.org/10.1140/epjd/e2009-00026-8
Muñoz-Navia MM, Dorantes-Dávila J, Zitoun D, Amiens C, Jaouen N, Rogalev A, Respaud M, Pastor GM (2009) Tailoring the magnetic anisotropy in corh nanoalloys. Appl Phys Lett 95(23):233,107. https://doi.org/10.1063/1.3272000
Panizon E, Ferrando R (2016) Strain-induced restructuring of the surface in core@shell nanoalloys. Nanoscale 8:15,911–15,919. https://doi.org/10.1039/C6NR03560D
Parr RG, Yang W (1989) Density-functional theory of atoms and molecules. Oxford University Press, Oxford, pp 186–194
Perdew JP (1991) Unified theory of exchange and correlation beyond the local density approximation. In: Ziesche P, Eschrig H (eds) Electronic structure of solids 91', vol 17. Akademie Verlag, Berlin, pp 11–20
Pianet V, Urdampilleta M, Colin T, Clérac R, Coulon C (2016) Magnetic tetrastability in a spin chain. Phys Rev B 94:054,431. https://doi.org/10.1103/PhysRevB.94.054431
Rau IG, Baumann S, Rusponi S, Donati F, Stepanow S, Gragnaniello L, Dreiser J, Piamonteze C, Nolting F, Gangopadhyay S, Albertini OR, Macfarlane RM, Lutz CP, Jones BA, Gambardella P, Heinrich AJ, Brune H (2014) Reaching the magnetic anisotropy limit of a 3d metal atom. Science 344(6187):988–992. https://doi.org/10.1126/science.1252841. http://science.sciencemag.org/content/344/6187/988.full.pdf
Rossi G, Ferrando R, Mottet C (2008) Structure and chemical ordering in copt nanoalloys. Faraday Discuss 138:193–210. https://doi.org/10.1039/B705415G
Ruiz-Díaz P, Stepanyuk VS (2014) Effects of surface charge doping on magnetic anisotropy in capping 3d/5d(4d) multilayers deposited on highly polarizable substrates. J Phys D Appl Phys 47(10):105,006. http://stacks.iop.org/0022-3727/47/i=10/a=105006
Ruiz-Díaz P, Dasa TR, Stepanyuk VS (2013) Tuning magnetic anisotropy in metallic multilayers by surface charging: an ab initio study. Phys Rev Lett 110:267,203. https://doi.org/10.1103/PhysRevLett.110.267203
Ruiz-Díaz P, Stepanyuk OV, Stepanyuk VS (2015) Effects of interatomic coupling on magnetic anisotropy and order of spins on metallic surfaces. J Phys Chem C 119(46):26,237–26,241. https://doi.org/10.1021/acs.jpcc.5b10211
Sahoo S, Hucht A, Gruner ME, Rollmann G, Entel P, Postnikov A, Ferrer J, Fernández-Seivane L, Richter M, Fritsch D, Sil S (2010) Magnetic properties of small Pt-capped Fe, Co, and Ni clusters: a density functional theory study. Phys Rev B 82:054,418. https://doi.org/10.1103/PhysRevB.82.054418
Schnur S, Groß A (2011) Challenges in the first-principles description of reactions in electrocatalysis. Catal Today 165(1):129–137. Theoretical Catalysis for Energy Production and Utilization: from First Principles Theory to Microkinetics
Serrate D, Yoshida Y, Moro-Lagares M, Kubetzka A, Wiesendanger R (2016) Spin-sensitive shape asymmetry of adatoms on noncollinear magnetic substrates. Phys Rev B 93:125,424. https://doi.org/10.1103/PhysRevB.93.125424
Singha A, Donati F, Wäckerlin C, Baltic R, Dreiser J, Pivetta M, Rusponi S, Brune H (2016) Magnetic hysteresis in trimers on Cu(111). Nano Lett 16(6):3475–3481. https://doi.org/10.1021/acs.nanolett.5b05214

Strasser P, Koh S (2010) Lattice-strain control of the activity in dealloyed core-shell fuel cell catalysts. Nat Chem 2:454–460. https://doi.org/10.1038/nchem.623

Sun S, Murray CB, Weller D, Folks L, Moser A (2000) Monodisperse fept nanoparticles and ferromagnetic fept nanocrystal superlattices. Science 287(5460):1989–1992. https://doi.org/10.1126/science.287.5460.1989. http://sciencemag.org/content/287/5460/1989

Wang D, Wu R, Freeman AJ (1993) First-principles theory of surface magnetocrystalline anisotropy and the diatomic-pair model. Phys Rev B 47:14,932–14,947. https://doi.org/10.1103/PhysRevB.47.14932

Yin S, Moro R, Xu X, de Heer WA (2007) Magnetic enhancement in cobalt-manganese alloy clusters. Phys Rev Lett 98:113,401